Hydrogen production by steam reforming of bio-oil/bio-ethanol mixtures in a continuous thermal-catalytic process

Aingeru Remiro*, Beatriz Valle, Lide Oar-Arteta, Andrés T. Aguayo, Javier Bilbao, Ana G. Gayubo

Chemical Engineering Department, University of the Basque Country, P. O. Box 644, 48080. Bilbao, Spain. Phone: +34 946 015361. Fax: +34 946 013 500

**email: aingeru.remiro@ehu.es*

Abstract

The feasibility of the steam reforming of bio-oil aqueous fraction and bio-ethanol mixtures has been studied in a continuous process with two in-line steps: thermal step at 300 ºC (for the controlled deposition of pyrolytic lignin during the heating of the bio-oil/bio-ethanol feed) followed by steam reforming in a fluidized bed reactor on a Ni/α-Al_2O_3 catalyst. The effect of bio-ethanol content in the feed has been analyzed in both the thermal and reforming steps, and the suitable range of operating conditions (temperature and space-time) has been determined for obtaining a high and steady hydrogen yield. Higher ethanol content in the mixture feed improves the reaction indices and reduces coke deposition. Operating conditions of 700 ºC and space-times higher than 0.23 $g_{catalyst}$ h $(g_{bio\text{-}oil+EtOH})^{-1}$ are suitable for attaining almost fully conversion of oxygenates (bio-oil and ethanol) and hydrogen yields above 93 %, with low catalyst deactivation.

Keywords: bio-oil, bioethanol, hydrogen production, steam reforming, fluidized reactor

1. Introduction

A biomass-based plant (bio-refinery) is the best solution to combine and integrate various processes for converting plant-based biomass to chemicals, energy and materials in order to maximize economic and environmental benefits, while minimizing waste and pollution [1]. Sultana and Kumar [2] found that the delivery cost of a feedstock that combines woody biomass and agricultural biomass is lower than that for a single type of biomass. Consequently, the joint valorization of oxygenated compounds derived from different types of biomasses, such as bio-oil and bio-ethanol (e.g. by catalytic steam reforming for obtaining H_2), is an interesting route for the development of the bio-refinery concept. Bio-oil is produced by fast pyrolysis of woody biomass, such as mill and harvest residues [3], and bio-ethanol can be sustainably obtained by hydrolysis/fermentation of agricultural lignocellulosic biomass [4,5].

The bio-oil is a complex mixture of water and oxygenated compounds (acids, alcohols, ketones, phenols, furans, etc.), whose composition depends on the biomass source and operating conditions of pyrolysis [6]. The viability of bio-oil reforming process is curtailed by the problems associated with re-polymerization of certain bio-oil components (i.e., derivatives of the lignin contained in biomass) that affect reactor operation and cause catalyst deactivation. These problems are mitigated with different strategies, such as the valorization of the bio-oil aqueous fraction, the previous separation of pyrolytic lignin and the co-feeding of methanol [7].

The lignocellulosic ethanol has a great potential as a chemical building block for bio-refineries [8] and its catalytic steam reforming avoids the costly dehydration steps required for other valorization strategies. Furthermore, its production cost has been significantly reduced due to advances in the conversion techniques [9].

Besides, bio-ethanol can replace the methanol commonly used to stabilize the bio-oil during its storage [10], which increases the interest of reforming this mixture.

The stoichiometry of the overall reactions for bio-oil and ethanol steam reforming are given by Eqs. (1) and (2), respectively:

$$C_nH_mO_k + (2n-k)H_2O \rightarrow nCO_2 + (2n+m/2-k)H_2 \quad (1)$$

$$C_2H_6O + 3H_2O \rightarrow 2CO_2 + 6H_2 \quad (2)$$

In practice, the hydrogen yield is lower than the stoichiometric maximum due to undesired secondary reactions (thermal decomposition of oxygenates, methanation, reverse-WGS reaction, ethanol dehydration or dehydrogenation).

Nickel-based catalysts have been widely used in the literature for reforming the aqueous fraction of bio-oil [11,12] and ethanol [13-15] due to the high C-C bond-breaking activity and the relatively low cost. Among oxide supports, Al_2O_3-based supports are often used as reforming catalysts because of their mechanical and chemical resistance [16].

This paper analyzes the feasibility of the steam reforming of bio-oil aqueous fraction and bio-ethanol mixtures on Ni/α-Al_2O_3 catalyst in a continuous process with two steps in line (thermal and catalytic) (Figure 1). This two-step system minimizes the problems inherent to the bio-oil catalytic valorization, caused by the deposition of carbonaceous solid (pyrolytic lignin) during feed preheating [17]. The effect bio-ethanol in the feed has on both the thermal and the reforming steps is analyzed and the suitable range of operating conditions (temperature and space-time) is determined for obtaining steady and high hydrogen yield.

Figure 1

2. Experimental

2.1. Preparation and characterization of bio-oil/bio-ethanol mixtures

Bio-oil was obtained by flash pyrolysis of pine sawdust in a semi-industrial demonstration plant located in Ikerlan-IK4 technology center (Alava, Spain), with a biomass feeding capacity of 25 kg/h [18]. The aqueous fraction (82 wt% water) was obtained by phase separation after adding water to the raw bio-oil in a water/bio-oil mass ratio = 2/1 [19]. For every 100 g of raw bio-oil (composed of 65 g of oxygenated compounds and 35 g water) two fractions are obtained: 15 g of organic fraction and 285 g of aqueous fraction. The bio-oil/bio-ethanol mixtures were prepared by adding aqueous ethanol (82 wt% water) to the bio-oil aqueous fraction in mass ratios ranging from 80/20 up to 20/80. In this paper the mixtures are denoted as B_x/E_y, where x is the percentage (wt%) of bio-oil aqueous fraction (B) and y is the percentage (wt%) of aqueous ethanol (E) in the mixture.

The composition of the raw bio-oil, the bio-oil aqueous fraction and the bio-oil/bio-ethanol mixture B_{50}/E_{50} (Table 1, on a dry basis) was determined by GC/MS analyzer (*Shimadzu QP2010S device*). Bio-ethanol addition to the bio-oil aqueous fraction only contributes to molecular dilution of the bio-oil oxygenates. The reactivity reported between light alcohols

and organic compounds [20] is not observed probably because the mixture is highly diluted in water (82 wt%). The difference between the ethanol content in the mixture B_{50}/E_{50} (52 wt%) and the nominal content (50 wt%) is caused by cumulative errors in the mixture preparation (a large quantity to conduct all experiments) and by the chromatographic analysis (the compounds with highest molecular weight are not detected).

Table 1

The elemental composition (C, H, O) of the raw bio-oil, bio-oil aqueous fraction and pyrolytic lignin deposited in the thermal step was determined by elemental analysis (*Leco CHN-932 analyzer* and ultra-microbalance *Sartorious M2P*). The resulting molecular formulas (on a dry basis) are $C_{4.3}H_{7.2}O_{2.6}$ and $C_{4.1}H_{7.4}O_{2.7}$, for the raw bio-oil and bio-oil aqueous fraction, respectively. The water content of (bio-oil aqueous fraction)/bio-ethanol mixtures (82 wt%) was quantified by Karl Fischer titration in a *870 KF Titrino Plus* device.

2.2. Catalyst

The α-Al_2O_3 support was obtained by calcining hydrated γ-Al_2O_3 (150-250 μm particle size) at 1100 ºC for 5 h. After the subsequent impregnation with $Ni(NO_3)_2 \cdot 6H_2O$ and drying at 110 °C for 24 h, the final calcination was carried out at 700 °C for 3 h. The nominal Ni content of the Ni/α-Al_2O_3 catalyst is 10 wt%. Although it has been found that conversion of oxygenates in the steam reforming increases with Ni content, a limited value of this content (10-15 wt%) is the best option, given that this low content minimizes Ni sintering problems at high temperature [21].

The catalyst was sieved (150-250 μm) and mixed with an inert solid (CSi carborundum, with 30-50 μm particle size) in a catalyst/inert mass ratio of 1/4, for improving fluid-dynamic properties of the catalytic bed and reducing axial dispersion. The CSi is a suitable material as diluent in fluidized bed reactors due to its high mechanical resistance and good thermal conductivity [22]. The particle sizes of both materials (of different density) were established in order to have isodromic particles (with similar minimum fluidization velocity). They were determined by means of a fluid-dynamic study (analyzing the evolution of pressure drop with gas linear velocity in a glass reactor at atmospheric pressure and room temperature). Furthermore, it was found that the mixture of both solids within the bed is uniform under the reaction conditions. The catalyst was reduced in the

reactor prior to each reforming reaction, under a H_2-He flow (5 vol % of H_2) for 2 h at 700 ºC.

The catalyst properties have been previously described in detail [23]. The physical properties, such as BET surface area (65.5 m^2/g), pore volume (0.174 cm^3/g) and average pore size (7.4 nm) have been determined from the N_2 adsorption-desorption isotherms, obtained by using a *Micromeritics ASAP 2010C* analyzer. This device was also used for hydrogen chemisorption measurements for quantifying nickel dispersion and specific metal surface area, with values being 2.1 % and 14.1 m^2/g_{metal}, respectively. Nickel content (8.93 wt%) was measured by inductively coupled plasma and atomic emission spectroscopy (ICP-AES). The X-ray diffraction (XRD) pattern measured on a *Bruker D8 Advance* diffractrometer with a $CuK_{\alpha 1}$ radiation showed diffraction lines corresponding to the reflection of Al_2O_3 phase and Ni^0 phase (at 2θ angles of 44.5º, 51.9º and 76.4º).

The coke deposited on the catalyst after each steam reforming reaction was quantified by temperature programmed oxidation (TPO), conducted in a *TA Instruments Q5000 IR* thermobalance coupled to a mass *Thermostar Balzers Instrument* spectrometer for monitoring the signal corresponding to CO_2 (mass 44).

2.3. Reaction system and operating conditions

The two-step reaction equipment has been previously described in detail for the steam reforming of aqueous bio-oil [23]. The first reactor (thermal processing of the feed) retains the carbonaceous solid (pyrolytic lignin) formed by re-polymerization of certain bio-oil oxygenated components. The volatile compounds leaving this thermal step are subsequently transformed (by catalytic steam reforming) in the second unit (fluidized bed reactor). The controlled deposition of pyrolytic lignin in a specific thermal step prior to the catalytic reactor minimizes the operating problems caused by this deposition and attenuates catalyst deactivation. This fact was previously verified for the catalytic conversion of raw bio-oil into hydrocarbons [24,25]. Besides, the use of a fluidized bed reactor favors a uniform gasification of the coke precursors adsorbed on the catalyst, thereby attenuating the catalyst deactivation [26].

The analysis of the reforming products was carried out on-line with a gas chromatograph (*Agilent Micro GC 3000*) provided with four modules for analysing the following: (1) permanent gases (O_2, H_2, CO, and CH_4) with 5A molecular sieve capillary column; (2) light oxygenates (C_{2-}), CO_2 and water, with Plot Q capillary column; (3) C_2-C_4

hydrocarbons, with alumina capillary column; (4) oxygenated compounds (C_{2+}) with Stabilwax type column.

The flow-rate of (bio-oil aqueous fraction)/bio-ethanol mixtures was 0.1 ml min^{-1} and was controlled by an injection pump *Harvard Apparatus 22.* The operating conditions were as follows: thermal step, 300 ºC; catalytic steam reforming, 500-800 ºC; steam-to-carbon ratio at the fluidized bed reactor inlet (S/C), 5.8-10; space-time, 0.10-0.45 $g_{catalyst}$ h $(g_{bio\text{-}oil+EtOH})^{-1}$ (water not included); gas hourly space velocity ($G_{C1}HSV$), 8200-41500 h^{-1} (calculated at the reaction temperature as CH_4 equivalent units) and time over frequency (TOF), 6.5-32.3 s^{-1}.

The particle size of the catalyst (150-250 μm) and the linear velocity of the gas under the reaction conditions (around 3.5 cm s^{-1}) are suitable for minimizing the limitations of internal and external diffusion, respectively. This aspect was proven by ensuring that the results were independent of the feed flow-rate for the same space-time. Furthermore, the α-Al_2O_3 support has a mesoporous structure that facilitates the diffusion of bio-oil compounds (with different molecular weights) within the pores. Consequently, the conditions set are suitable for fluidization and for reducing diffusional limitations.

2.4. Reaction indices

The bio-oil and bio-ethanol conversion are calculated by Eq. (4), considering their molar flow-rates (as C units contained) at the inlet, $F_{j,inlet}$, and outlet (un-reacted bio-oil or ethanol), F_j, of the catalytic reactor:

$$X_j = \frac{F_{j,inlet} - F_j}{F_{j,inlet}} \times 100 \quad (4)$$

The molar flow-rate of the bio-oil fed into the two-unit system is calculated from its mass flow-rate and empirical formula ($C_{4.1}H_{7.4}O_{2.7}$). The molar flow-rate of the bio-oil at the catalytic reactor inlet ($F_{bio\text{-}oil,inlet}$) is determined from a mass balance in each run by considering the amount of PL deposited in the thermal unit and its elemental composition (Figure 2).

The molar flow-rate of the bio-oil at the reactor outlet ($F_{bio\text{-}oil}$) is calculated from the total mole number at the reactor outlet (quantified by a mass balance to the catalytic reactor) and the molar fraction of oxygenates (excluding ethanol), analyzed by μGC and GC/MS.

The hydrogen yield is calculated by Eq. (5) as a percentage of the maximum allowed by stoichiometry, considering the contribution of both reactants (bio-oil and bio-ethanol), according to Eqs. (1) and (2).

$$Y_{H_2} = \frac{F_{H_2}}{((2 + m/(2n) - k/n)\, F_{\text{bio-oil,inlet}} + 3F_{\text{EtOH,inlet}})} \times 100 \quad (5)$$

where F_{H2} is the molar flow of H_2 obtained.

The yield of each carbon-containing byproduct (CO_2, CO, CH_4 and C_2-C_4 light hydrocarbons) is quantified by Eq. (6), based on the total C fed into the catalytic reactor (taking into account both the bio-oil aqueous fraction and the bio-ethanol):

$$Y_i = \frac{F_i}{\left(F_{\text{bio-oil,inlet}} + F_{\text{EtOH,inlet}}\right)} \times 100 \quad (6)$$

where F_i is the molar flow of each *i* product.

The selectivity of each product is calculated by Eq. (7):

$$S_i = \frac{F_i}{\Sigma F_i} \times 100 \quad (7)$$

where ΣF_i is the sum of gaseous products (excluding oxygenated compounds and water) at the reactor outlet.

The experimental errors determined by repeated experiments are ± 3 % in the H_2 yield values and ± 1 % in those of C-containing products.

The following sections deal with the features of the steam reforming of bio-oil aqueous fraction and bio-ethanol mixtures by analyzing the effect bio-ethanol content in the feed and operating conditions (reforming temperature and space-time) have on the hydrogen yield and catalyst deactivation.

3. Results and discussion

3.1. Effect of co-feeding ethanol on pyrolytic lignin deposition in the thermal step

The effect bio-ethanol content of the mixture fed into the two-unit system has on the deposition of pyrolytic lignin (in the first thermal unit) was analyzed. Accordingly, the pyrolytic lignin yield (PL yield) formed by re-polymerization of the bio-oil fed was

quantified using Eq. (3). The bio-ethanol is not considered for this calculation because it does not undergo re-polymerization.

$$\text{PL yield}(\text{wt\%}) = \frac{\text{pyrolytic lignin deposited (g)}}{\text{oxygenates in bio - oil fed (g)}} \times 100 \quad (3)$$

The PL yield and its elemental composition for different bio-ethanol contents in the mixture fed are shown in Figure 2. These results reveal that the addition of aqueous ethanol (bio-ethanol) to the bio-oil aqueous fraction slightly attenuates the re-polymerization of bio-oil oxygenates and so pyrolytic lignin deposition in the thermal unit. Besides, an increase in bio-ethanol content does not significantly affect pyrolytic lignin composition (only a slight increase in O content and a decrease in C content is observed). These results suggest that the slight attenuation of pyrolytic lignin deposition is a consequence of molecular dilution, which changes the microstructure of the bio-oil emulsion.

The attenuation of lignin deposition observed for these mixtures is lower than that previously observed for raw bio-oil/methanol mixtures [27]. This is probably due to the removal of the fraction containing high molecular weight oxygenates from the raw bio-oil for obtaining the bio-oil aqueous fraction used in this work. This suggests that the stabilizing effect of the alcohol (ethanol or methanol) is more significant when it is added to the raw bio-oil, given that it is a more unstable emulsion than the bio-oil aqueous fraction.

Figure 2

3.2. Catalytic steam reforming of (bio-oil aqueous fraction)/bio-ethanol mixtures

3.2.1. Effect of feed composition

Fig. 3 shows the results of evolution with time on stream of bio-oil and ethanol conversion and the yield of H_2, CO and CH_4 in the steam reforming of bio-oil aqueous fraction (B_{100}, Fig. 3a), a 50 wt% mixture of (bio-oil aqueous fraction)/bio-ethanol (B_{50}/E_{50}, Fig. 3b) and bio-ethanol (E_{100}, Fig. 3c). Based on these runs the possible differences between the joint reforming of bio-oil and bio-ethanol and their individual reforming are analyzed. The reforming conditions were as follows: 700 ºC; space-time, 0.1 $g_{catalyst}$ h $(g_{bio\text{-}oil+EtOH})^{-1}$; $G_{C1}HSV$, 41500 h^{-1}; Q_{feed}, 0.1 ml $(min)^{-1}$.

Figure 3

It is observed that bio-oil conversion at zero time on stream (fresh catalyst) is almost full for B_{100} (Fig. 3a) and B_{50}/E_{50} (Fig. 3b) feeds and slightly decreases with time on stream. Bio-ethanol conversion remains full and steady for 5 h reaction for B_{50}/E_{50} (Fig. 3b) and E_{100} (Fig. 3c) feeds. Besides, B_{100} and E_{100} feeds yield 84 % and 91 % H_2, respectively, at zero time on stream, whereas B_{50}/E_{50} feed has a halfway behavior between the individual feeds, with H_2 yield being 89 %. The CO yield obtained from the reforming of B_{100} (≈ 10 %) is lower than that from E_{100} (≈ 22 %) and an intermediate yield (19 %) is obtained for B_{50}/E_{50} feed. The initial yield of CH_4 is low and very similar for the three feeds studied (≈ 2 %).

These results at zero time on stream evidence the different reaction mechanism for the steam reforming of bio-oil and ethanol. A reaction pathway has been suggested for ethanol steam reforming which includes as follows [28,29]: 1) ethanol dehydrogenation to acetaldehyde, 2) acetaldehyde decomposition to produce CO + CH_4 and 3) WGS reaction and CH_4 reforming to produce hydrogen. According to this, the higher production of CO at zero time on stream obtained in the ethanol reforming may be a consequence of acetaldehyde decomposition and the reforming reaction of the CH_4 produced in this decomposition.

H_2 and CO_2 yields decrease and that of CO increases with time on stream for all the feeds in Fig. 3, while the conversion of bio-oil and ethanol decreases and that of CH_4 increases in a less pronounced way with time on stream. This fact reveals that the WGS reaction is affected more severely by the catalyst deactivation than oxygenates reforming and decomposition reactions. The decrease in H_2 and CO_2 yield and the increase in CO yield with time on stream are more significant for B_{100} feed (Fig. 3a) than for E_{100} feed (Fig. 3c), whereas B_{50}/E_{50} feed behavior is halfway between those for the individual feeds (Fig. 3b). Catalyst deactivation also affects CH_4 reforming, whose yield increases with time on stream, with this effect being more noticeable for B_{100} feed (from 1 % up to 9 %) than for E_{100} (from 2 % up to 4 %). These results reveal that the catalyst undergoes lower deactivation by feeding ethanol.

The catalyst deactivation in bio-ethanol reforming is caused by Ni site blockage by coke, whose formation is enhanced by the presence in the reaction medium of byproducts, such as ethylene (following oligomerization), methane (dehydrogenation) and (CO Boudouard reaction) [30]. Remiro et al. [26] have proposed a mechanism for coke formation in bio-oil reforming, identifying the steps of coke formation from by-products. They also concluded

that the coke formation capability increases as the reforming activity of the catalyst decreases. For both feeds catalyst deactivation by coke is attenuated under conditions enhancing the reforming/gasification of coke precursors and the formation of filamentous coke instead of encapsulating coke.

In order to analyze in more detail the effect of bio-ethanol content in the feed, the steam reforming of B_X/E_Y mixtures with different mass ratios was carried out (under the same operating conditions as in Fig. 3). Table 2 shows the results obtained for bio-oil and ethanol conversion (X_i), H_2 yield in the reforming unit (Y_{H2}) and selectivity of reaction products (S_i) at zero time on stream and after 5 h reaction, and the coke content deposited on the catalyst after each reaction (C_c). The overall H_2 yield $(Y_{H2})^G$ by mass unit of the bio-oil and bio-ethanol fed into the two-step system was also estimated.

Table 2

Bio-ethanol conversion is independent of the feed composition and is almost full throughout 5 h reaction, whereas bio-oil conversion decreases by 10 % and 2 % after 5 h reaction for B_{100} and B_{20}/E_{80} feeds, respectively (Table 2). The initial H_2 yield increases significantly when 20 wt% bio-ethanol is added to the bio-oil aqueous fraction (from 84.4 % to 88.2 % for B_{80}/E_{20} feed), with this increase being attenuated for higher contents of bio-ethanol (91 % for E_{100} feed). Besides, the decrease in H_2 yield after 5 h time on stream (caused by catalyst deactivation) steadily attenuates by increasing the amount of ethanol in the feed, thus H_2 yield decreasing to 35 % for B_{100} feed and to 79 % for B_{20}/E_{80}. Moreover, the difference observed between the H_2 yield obtained in the reforming reactor (Y_{H2}) and the overall H_2 yield in the two-step system, $(Y_{H2})^G$, is lower as the bio-ethanol content in the feed is higher. This should be attributed to the lower deposition of pyrolytic lignin in the thermal step (due to the lower content of bio-oil in the mixture).

The evolution of hydrogen selectivity (S_{H2}) with the bio-ethanol content in the feed follows a similar trend to the H_2 yield: the initial value is higher as bio-ethanol content is increased (although less pronounced than for yield) and then goes on to decrease with time on stream in a less pronounced way as the bio-ethanol content increases.

The initial selectivity of CO increases steadily with the bio-ethanol content in the feed and that of CO_2 decreases. The initial selectivity of CH_4 is less affected by the bio-ethanol/bio-oil ratio in the feed. The selectivity of CO and CH_4 increases with time on stream due to catalyst deactivation affecting mainly the WGS and CH_4 reforming reactions. This increase

(and thus deactivation) is considerably attenuated by increasing the ethanol content in the feed. This result suggests a higher contribution of bio-oil oxygenate compounds than bio-ethanol to the catalyst deactivation by coke deposition. The results of coke content deposited for the different feeds (Table 2) confirm this hypothesis.

The results in Fig. 3 and Table 2 reveal that bio-ethanol addition has a favorable effect on the bio-oil aqueous fraction reforming because it provides stability by attenuating catalyst deactivation by coke and enhancing a high and steady hydrogen production. Moreover, Table 2 data show that the presence of ethanol in the reaction medium has a beneficial synergistic effect of attenuating coke deposition. Thus, the coke content obtained in the reforming of the B_{50}/E_{50} mixture is 1.3 wt%, which is lower than the theoretical content (2.15 wt%) that would correspond to the contribution of all components in the feed. This result is caused by a change in coke precursors concentrations in the reaction medium.

Furthermore, it should be considered that the limited internal diffusion of the bio-oil heaviest compounds may contribute to a lower conversion and to a different distribution of the reaction products obtained from the different feeds, which will be more significant at high temperature. The relevance of support diffusivity on the diffusional limitations in ethanol reforming has been reported in the literature (by the Weisz-Prater criterion). This limitation is significant above 350 °C for a $Ni/MgAl_2O_4$ catalyst [31] but for a Ni/Al_2O_3 catalyst (similar to that used in this paper) there is no diffusional limitation [21] due to the diffusing capacity within the Al_2O_3 support. However, this paper studies the joint reforming of ethanol and the oxygenated mixture constituting the bio-oil, so that the diffusional limitation is presumably heterogeneous and may affect the bio-oil compounds of high molecular weight.

3.2.2. Effect of reforming temperature

The runs were performed in the 500-800 ºC range, at low space-time (0.1 $g_{catalyst}$ h $(g_{bio\text{-}oil+EtOH})^{-1}$) and by feeding the mixture of 50 wt% bio-oil aqueous fraction and bio-ethanol (B_{50}/E_{50}). For this feed, 23.7 wt% of pyrolytic lignin (PL) is retained in the thermal step, whose elemental composition is 65.3 wt% C, 4.9 wt% H and 29.8 wt% O (Figure 2). Consequently, the composition of the treated bio-oil that enters the catalytic reactor is $C_{3.7}H_{8.2}O_{3.0}$ and thereby, 2.3 mol of H_2 can be obtained from each mol of C in the bio-oil. The bio-ethanol contained in the feed can be converted to 3 mol of H_2 for every mol of C.

Fig. 4 shows the results at zero time on stream (fresh catalyst, continuous lines) and after 5 h reaction (dashed lines) of bio-oil and bio-ethanol conversion (Fig. 4a), H_2 yield and selectivity (Fig. 4b), CO and CO_2 yields (Fig. 4c) and CH_4 yield (Fig. 4d). HC yield (mainly ethylene and ethane) is not shown because is lower than 1 % in all cases.

Figure 4

Fig. 4a shows that ethanol conversion increases significantly with temperature, being almost full at 700 ºC, whereas the increase in bio-oil conversion with temperature is less pronounced and temperatures above 800 ºC are required for achieving full conversion of bio-oil with this low value of space-time. The yields of H_2 (Fig. 4b) and CO_2 (Fig. 4c) at zero time on stream follow similar trends with temperature, with both yields increasing significantly from 500 to 600 ºC and going through a maximum at 700 ºC. The slight decrease in these yields above 700 ºC is caused by the reverse-WGS reaction, which is thermodynamically favored at higher temperature, as evidenced by the progressive increase in the CO yield with temperature (Fig. 4c). The low CO yield is a consequence of the catalyst activity for the WGS reaction. The low initial yield of CH_4 (≈ 2 %) (Fig. 4d) is a consequence of: i) a more effective competition of oxygenate catalytic reforming reactions than thermal decomposition reactions and ii) the effective CH_4 reforming at the temperature range studied.

The conversion of both bio-oil aqueous fraction and bio-ethanol decrease after 5 h time on stream due to catalyst deactivation, which is notably attenuated by increasing temperature (Fig.4a). The deactivation is severe at 600 ºC, so that bio-oil and ethanol conversion decreases by 40 % and 22 %, respectively. The yields of H_2 (Fig. 4b) and CO_2 (Fig. 4c) also undergo significant reduction with time on stream, whereas the yields of CO and CH_4 remain almost constant. At 700 ºC and 800 ºC, the decrease in bio-oil and ethanol conversion after 5 h time on stream is very low. However, the decrease in H_2 and CO_2 yields is noticeable at both temperatures. It should be noted that the values for H_2 and CO_2 yield after 5 h reaction show a peak at 700 ºC. Moreover, the values of H_2 selectivity after 5 h reaction progressively decrease with temperature (Fig. 4b) due to the increase in the yield of CO (Fig. 4c) and CH_4 (Fig. 4d), which is significant above 700 ºC.

The aforementioned results evidence that deactivation selectively affects to the different steps of the reaction scheme. The decrease in bio-oil conversion and the fact that at 600 ºC CO yield remains constant after 5 h reaction reveal that both the oxygenate reforming

reaction and the WGS reaction are similarly affected by deactivation at this relatively low temperature. Nevertheless, the increase in CO yield after 5 h reaction at 700 ºC and 800 ºC evidences that catalyst deactivation affects more severely WGS reaction than oxygenate reforming reactions at high temperatures. Deactivation significantly influences the reforming reaction of oxygenates at 800 ºC, which favors thermal cracking reactions leading to CH_4 and CO. CH_4 reforming is also strongly affected by deactivation at high temperatures, which contributes to the great increase in CH_4 yield observed at 800 ºC after 5 h time on stream (Fig. 4d). Furthermore, the thermodynamics of WGS reaction is hindered by increasing temperature.

The results of coke content deposited on the catalyst after 5 h reaction at the different temperatures are set out in Table 3. As observed, coke deposition on the catalyst (and thus catalyst deactivation) reduces as temperature is increased by enhancing the gasification reactions involving the coke deposited [26]. These results are consistent with those in Fig. 4, where a significant deactivation is observed at temperatures below 700 °C. The loss of catalyst activity observed at 800 ºC is not due to coke deposition, which is negligible at this temperature, but to the sintering of the metallic function as proven in previous works [23,26]. It was found that the Ni crystal size of the catalyst used at 700 °C and regenerated by coke combustion is the same as that of the fresh catalyst (8 nm), thus confirming that the only cause of deactivation at this temperature is coke deposition. However, Ni sintering is remarkable at 800 °C and the Ni particle size of the catalyst used at this temperature is 15 nm (after removing the coke). Accordingly, 700 °C is a suitable temperature for minimizing deactivation and avoiding metal sintering, which allows the catalyst to be used continuously in reaction-regeneration cycles.

Table 3

Based on the above results, the optimum temperature for reforming mixtures of bio-oil and bio-ethanol is 700 °C, since at this temperature the maximum H_2 yield is attained with low deactivation of the Ni/α-Al_2O_3 catalyst after 5 h reaction. This stability is promoted by coke gasification (which is low below 700 ºC) and the low Ni metal sintering (which is significant above 700 °C).

3.2.3. Effect of space-time

The effect of space-time was analyzed at 700 ºC in the 0.1-0.5 $g_{catalyst}$ h $(g_{bio\text{-}oil+EtOH})^{-1}$ range, which corresponds to a gas hourly space velocity ($G_{C1}HSV$) between 8200 and

41500 h^{-1} and TOF between 6.5 and 32.3 s^{-1} feeding the B_{50}/E_{50} mixture. Fig. 5 shows the results at zero time on stream (fresh catalyst, continuous lines) and after 5 h reaction (dashed lines) for bio-oil and ethanol conversion (Fig. 5a), H_2 yield and selectivity (Fig. 5b), CO_2 and CO yields (Fig. 5c) and CH_4 yield (Fig. 5d).

Figure 5

An increase in space-time enhances the reforming reactions of both bio-oil and ethanol, thus increasing their conversion (Fig. 5a) and also the WGS reaction extent, as derived from the progressive decrease in the initial values of CO yield (Fig. 5c). An increase in space-time to 0.23 $g_{catalyst}$ h $(g_{bio\text{-}oil+EtOH})^{-1}$ results in a slight increase in the initial values of H_2 (Fig. 5b) and CO_2 (Fig. 5c) yields and enhancement of CH_4 reforming reaction (Fig. 5d). Nevertheless, a subsequent increase in space-time to 0.5 $g_{catalyst}$ h $(g_{bio\text{-}oil+EtOH})^{-1}$ does not significantly improve conversion and H_2 yield.

The decrease with time on stream in oxygenate conversion (Fig. 5a) and H_2 yield (Fig. 5b) is noticeable at space-times below 0.23 $g_{catalyst}$ h $(g_{bio\text{-}oil+EtOH})^{-1}$. For higher values of space-time, both oxygenate conversion and the H_2 yield hardly decrease in 5 h time on stream. CO yield increases from 19 % to 34 % for 0.1 $g_{catalyst}$ h $(g_{bio\text{-}oil+EtOH})^{-1}$ (Fig. 5c) due to the deactivation of the WGS reaction. The increase in CH_4 yield with time on stream to 9 % for the lowest value of space-time studied is explained by the cracking reactions to give CH_4 and CO, which are favored by catalyst deactivation (lower activity for the reforming reactions). In addition, the catalyst deactivation affects CH_4 reforming reaction (Fig. 5d), which contributes to significantly decreasing H_2 yield (Fig. 5b).

These kinetic results are consistent with the coke contents deposited on the catalyst for the different values of space-time (Table 4), i.e., they significantly decrease as space-time is increased.

Table 4

Based on the above results under the operating condition studied, a space-time of 0.23 $g_{catalyst}$ h $(g_{bio\text{-}oil+EtOH})^{-1}$ is enough for achieving high conversion of reactants in the (bio-oil aqueous fraction)/bio-ethanol mixture, with the maximum yield and selectivity of H_2 and low deactivation of the catalyst along 5 h reaction.

Furthermore, it should be noted that many of the afore-mentioned results correspond to severe deactivation conditions, and therefore they are useful to assess clearly the effect of operating conditions and bio-ethanol co-feeding on the deactivation and also to delimit the

range of conditions suitable for minimizing catalyst deactivation. The deactivation is also attenuated by using the proposed two-step reaction equipment, which facilitates the separation of compounds that repolymerize as pyrolytic lignin (in the first step), thus avoiding their deposition on the catalyst. Bearing in mind scaling up, the two-step process allows continuous operation, which may be performed without interruption by using a fluidized reactor with circulating catalyst. The partially deactivated catalyst would be fed back to the reactor after being regenerated in an external unit (for coke combustion). This technology is currently implemented for the conversion of methanol into olefins (MTO process) and has been proposed for the catalytic pyrolysis of biomass [32].

4. Conclusions

The joint steam reforming of the bio-oil aqueous fraction and bio-ethanol over a Ni/α-Al_2O_3 catalyst is a promising route for obtaining H_2 from two different biomass-derived feedstocks. Bio-ethanol addition promotes the steam reforming of the bio-oil aqueous fraction by slightly attenuating the pyrolytic lignin deposition (during bio-oil heating) and stabilizing the steam reforming reaction by decreasing the catalyst deactivation by coke, given that the composition of reaction medium hinders coke formation. The reaction system with two in-line steps (thermal and catalytic) is suitable to avoid pyrolytic lignin deposition in the fluidized bed reforming reactor, and therefore longer reactions may be carried out with low catalyst deactivation under suitable reaction conditions.

Operating conditions of 700 °C and space-times higher than 0.23 $g_{catalyst}h(g_{bio\text{-}oil+EtOH})^{-1}$ are suitable for reforming the bio-oil aqueous fraction and bio-ethanol mixture (50 wt%), given that almost full oxygenate conversion and a high hydrogen yield (above 93 %) are attained with low catalyst deactivation. The catalyst used at 700 °C fully recovers its activity after being regenerated by coke combustion.

Acknowledgments

This work was carried out with the financial support of the Department of Education Universities and Investigation of the Basque Government (IT748-13), the University of the Basque Country (UFI 11/39) and the Ministry of Economy and Competitiveness of the Spanish Government (Project CTQ2012-13428/PPQ). We appreciate the contribution of Ikerlan-IK4 Technology Centre to this paper.

Nomenclature

C_c coke content, wt %

$F_{j,inlet}$ molar flow rate of *j* (aqueous bio-oil or ethanol) at the reactor inlet, in C equivalent units, mol h^{-1}

F_j molar flow rate of *j* (aqueous bio-oil or ethanol) at the reactor outlet, in C equivalent units, mol h^{-1}

F_i molar flow rate of *i* product (H_2, CO, CO_2, CH_4, C_2-C_4) at the reactor outlet, mol h^{-1}

$G_{C1}HSV$ gas hourly space velocity, in CH_4 equivalent units, h^{-1}

PL pyrolytic lignin deposited in the thermal unit, wt%

Q_{feed} feed flow rate, ml min^{-1}

S/C steam-to-carbon ratio

S_i selectivity of *i* product (H_2, CO, CO_2, CH_4, C_2-C_4), %

X_j conversion of *j* (bio-oil and bio-ethanol), %

Y_{H2} hydrogen yield in the catalytic reforming step, %

$(Y_{H2})^G$ overall hydrogen yield in the two-unit system, %

Y_i yield of *i* product (H_2, CO, CO_2, CH_4, C_2-C_4), %

τ space-time, $g_{catalyst}$ h $(g_{bio\text{-}oil+EtOH})^{-1}$(water not included)

References

[1] Luo L, van der Voet E, Huppes G. Biorefining of lignocellulosic feedstock – Technical, economic and environmental considerations. Bioresour. Technol. 2010; 101:5023-32.

[2] Sultana A, Kumar A. Optimal configuration and combination of multiple lignocellulosic biomass feedstocks delivery to a biorefinery. Bioresour. Technol. 2011; 102:9947-56.

[3] Meier D, van de Beld B, Bridgwater AV, Elliott C, Oasmaa A, Preto F. State-of-the-art of fast pyrolysis in IEA bioenergy member countries. Renew. Sust. Energ. Rev. 2013; 20:619-41.

[4] FitzPatrick M, Champagne P, Cunningham MF, Whitney RA. A biorefinery processing perspective: Treatment of lignocellulosic materials for the production of value-added products. Bioresour. Technol. 2010; 101:8915-22.

[5] Hasunuma T, Okazari F, Okai N, Hara KY, Ishii J, Kondo A. A review of enzymes and microbes for lignocellulosic biorefinery and the possibility of their application to consolidated bioprocessing technology. Bioresour. Technol. 2013; 135:513-22.

[6] Oasmaa A, Meier D. Norms and standards for fast pirólisis liquids: 1. Round robin test. J. Anal. Appl. Pyrolysis 2005; 73:323-34.

[7] Trane R, Dahl S, Skjøth-Rasmussen MS, Jensen AD. Catalytic steam reforming of bio-oil. Int. J. Hydrogen Energy 2012; 37:6447-72.

[8] Posada JA, Patel AD, Roes A, Blok K, Faaij APC, Patel MK. Potential of bioethanol as a chemical building block for biorefineries: Preliminary sustainability assessment of 12 bioethanol-based products. Bioresour. Technol. 2013; 135:490-99.

[9] Viikari L, Vehmaanpera J, Koivula A. Lignocellulosic ethanol: From science to industry. Biomass Bioenergy 2012; 46:13-24.

[10] Oasmaa A, Kuoppala E, Selin JF, Gust S, Solantausta Y. Fast Pyrolysis of Forestry Residue and Pine. 4. Improvement of the Product Quality by Solvent Addition. Energy Fuels 2004; 18:1578-83.

[11] Medrano JA, Oliva M, Ruiz J, García L, Arauzo J. Hydrogen from aqueous fraction of biomass pyrolysis liquids by catalytic steam reforming in fluidized bed. Energy 2011; 36:2215-24.

[12] Yan CF, Cheng FF, Hu RR. Hydrogen production from catalytic steam reforming of bio-oil aqueous fraction over Ni/CeO_2ZrO_2 catalysts. Int. J. Hydrogen Energy 2010; 35:11693-99.

[13] Vizcaino AJ, Arena P, Baronetti G, Carrero A, Calles JA, Laborde MA, Amadeo N. Ethanol steam reforming on Ni/Al_2O_3 catalysts: Effect of Mg addition. Int. J. Hydrogen Energy 2008; 33:3489-92.

[14] Han SJ, Bang Y, Yoo J, Seo JG, Song IK. Hydrogen production by steam reforming of ethanol over mesoporous Ni–Al_2O_3–ZrO_2 xerogel catalysts: Effect of nickel content. Int. J. Hydrogen Energy 2013; 38:8285-92.

[15] Devianto H, Li ZL, Yoon SP, Han J, Nam SW, Lim TH, Lee HI. The effect of Al addition on the prevention of Ni sintering in bio-ethanol steam reforming for molten carbonate fuel cells. Int. J. Hydrogen Energy 2010; 35:2591-96.

[16] Roy B, Martinez U, Loganathan K, Datye AK, Leclerc CA. Effect of preparation methods on the performance of Ni/Al_2O_3 catalysts for aqueous-phase reforming of ethanol: Part I-catalytic activity. Int. J. Hydrogen Energy 2012; 37:8143-53.

[17] Gayubo AG, Valle B, Aguayo AT, Olazar M, Bilbao J. Pyrolytic lignin removal for the valorization of biomass pyrolysis crude bio-oil by catalytic transformation. J. Chem. Technol. Biotechnol. 2010; 85:132-44.

[18] Fernandez-Akarregi AR, Makibar J, Lopez G, Amutio M, Olazar M. Design and operation of a conical spouted bed reactor pilot plant (25 kg/h) for biomass fast pyrolysis. Fuel Process. Technol. 2013; 112:48-56.

[19] Czernik S, French R, Feik C, Chornet E. Hydrogen by catalytic steam reforming of liquid byproducts from biomass thermoconversion processes. Ind. Eng. Chem. Res. 2002; 41:4209-15.

[20] Bhattacharya P, Hassan EB, Steele P, Cooper J, Ingram L. Effect of acid catalysts and accelerated aging on the reaction of methanol with hydroxyacetaldehyde in bio-oil. Bioresources 2010; 5:908-19.

[21] Goyal N, Pant KK, Gupta R. Hydrogen production by steam reforming of model bio-oil using structured Ni/Al_2O_3 catalysts. Int. J. Hydrogen Energy 2013; 38:921-933.

[22] Pérez-Ramírez J, Berger RJ, Mul G, Kapteijn F, Moulijn JA. The six-flow reactor technology. A review on fast catalyst screening and kinetic studies. Catal. Today 2000; 60:93-109.

[23] Valle B, Remiro A, Aguayo AT, Bilbao J, Gayubo AG. Catalysts of $Ni/\alpha\text{-}Al_2O_3$ and $Ni/La_2O_3\text{-}\alpha Al_2O_3$ for hydrogen production by steam reforming of bio-oil aqueous fraction with pyrolytic lignin retention. Int. J. Hydrogen Energy 2013; 38:1307-18.

[24] Gayubo AG, Valle B, Aguayo AT, Olazar M, Bilbao J. Olefin production by catalytic transformation of crude bio-oil in a two-step process. Ind. Eng. Chem. Res. 2010; 49:123-31.

[25] Valle B, Gayubo AG, Aguayo AT, Olazar M, Bilbao J. Selective production of aromatics by crude bio-oil valorization with a nickel-modified HZSM-5 zeolite catalyst. Energy Fuels 2010; 24:2060-70.

[26] Remiro A, Valle B, Aguayo AT, Bilbao J, Gayubo AG. Operating conditions for attenuating $Ni/La_2O_3\text{-}\alpha Al_2O_3$ catalyst deactivation in the steam reforming of bio-oil aqueous fraction. Fuel Process. Technol. 2013; 115:222-32.

[27] Gayubo AG, Valle B, Aguayo AT, Olazar M, Bilbao J. Attenuation of catalyst deactivation by cofeeding methanol for enhancing the valorisation of crude bio-oil. Energy Fuels 2009; 23:4129-36.

[28] Ni M, Leung DYC, Leung MKH. A review on reforming bio-ethanol for hydrogen production. Int. J. Hydrogen Energy 2007; 32:3952-91.

[29] Navarro RM, Peña MA, Fierro JLG. Hydrogen production reactions from carbon feedstocks: Fossil fuels and biomass. Chem. Rev. 2007; 107:3952-91.

[30] Xu W, Liu Z, Johnston-Peck AC, Senanayake SD, Zhou G, Stacchiola D, Stach EA, Rodriguez JA. Steam reforming of ethanol on Ni/CeO_2: Reaction pathway and interaction between Ni and the CeO_2 support. ACS Catal. 2013; 3:975-84.

[31] Szijjártó GP, Pászti Z, Sajó I, Erdöhelyi A, Radnóczi G, Tompos A. Nature of the active sites in Ni/$MgAl_2O_4$-based catalysts designed for steam reforming of ethanol. J. Catal. 2013; 305:290-306.

[32] Jae J, Coolman R, Mountziaris TJ, Huber GW. Catalytic fast pyrolysis of lignocellulosic biomass in a process development unit with continual catalyst addition and removal. Chem. Eng. Sci. http://dx.doi.org/10.1016/j.ces.2013.12.023

Figure Captions

Figure 1. Hydrogen production layout according to the joint steam reforming of bio-oil and bio-ethanol obtained from biomass.

Figure 2. Effect of ethanol content in the feed on the amount (wt%) and elemental composition of the pyrolytic lignin (PL) deposited in the thermal step at 300 ºC.

Figure 3. Evolution with time on stream of oxygenate conversion and product yields. Reaction conditions: 700 ºC; S/C, 10; space-time, 0.1 $g_{catalyst}$ h $(g_{bio\text{-}oil+EtOH})^{-1}$; $G_{C1}HSV$, 41500 h^{-1}. Graph a: feed, B_{100}; Graph b: feed B_{50}/E_{50}; Graph c: feed, E_{100}.

Figure 4. Effect of temperature on the values at zero time on stream (fresh catalyst) and after 5 h reaction for bio-oil and ethanol conversions (a), H_2 yield and selectivity (b), CO and CO_2 yields (c), and CH_4 yield (d). Reaction conditions: feed, B_{50}/E_{50}; S/C, 7; space-time, 0.1 $g_{catalyst}$ h $(g_{bio\text{-}oil+EtOH})^{-1}$; $G_{C1}HSV$, 41500 h^{-1}.

Figure 5. Effect of space-time on the values at zero time on stream (fresh catalyst) and after 5 h reaction for bio-oil and ethanol conversions (a), H_2 yield and selectivity (b), CO and CO_2 yields (b), and CH_4 yield (d). Reaction conditions: feed B_{50}/E_{50}; 700 ºC; S/C, 7.

FIGURES

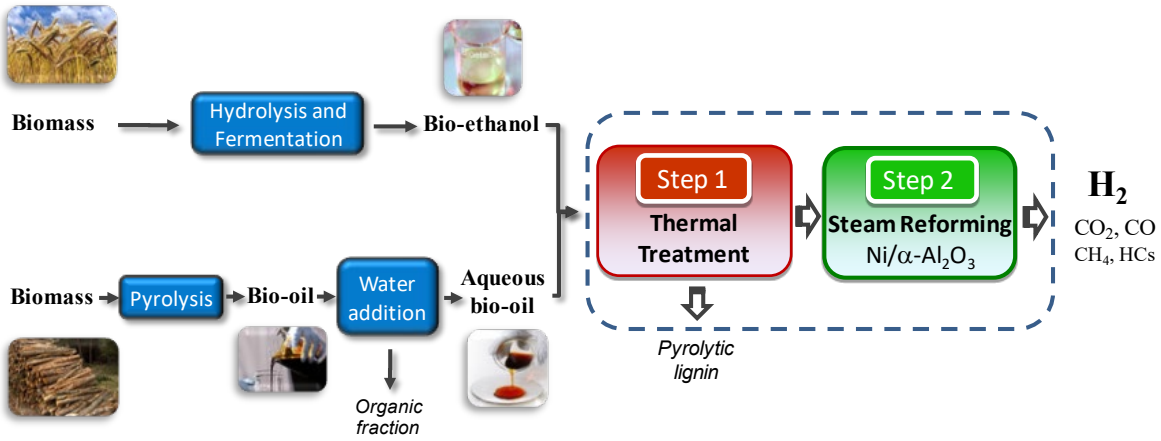

Figure 1

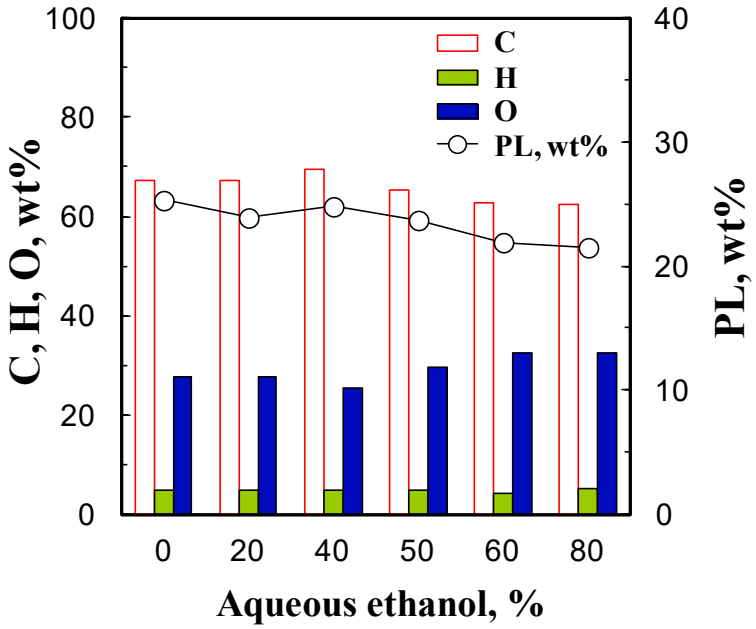
C
H
O
PL, wt%
C, H, O, wt%
PL, wt%
Aqueous ethanol, %
0
20
40
50
60
80
100
80
60
40
20
0
40
30
20
10
0

Figure 2

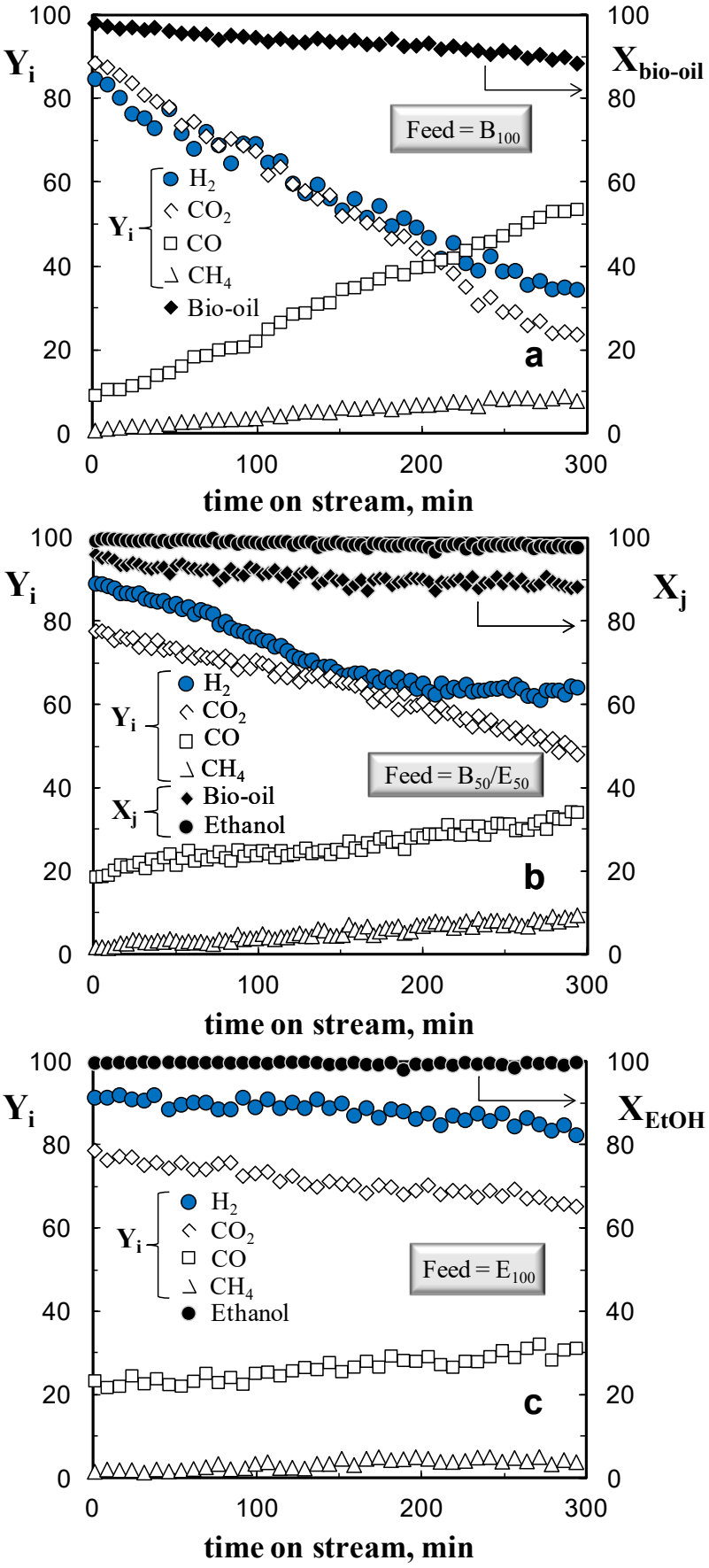
Y_i
X_bio-oil
Feed = B100
H2
CO2
CO
CH4
Bio-oil
a
time on stream, min
Y_i
X_j
Feed = B50/E50
H2
CO2
CO
CH4
Bio-oil
Ethanol
b
time on stream, min
Y_i
X_EtOH
Feed = E100
H2
CO2
CO
CH4
Ethanol
c
time on stream, min

Figure 3

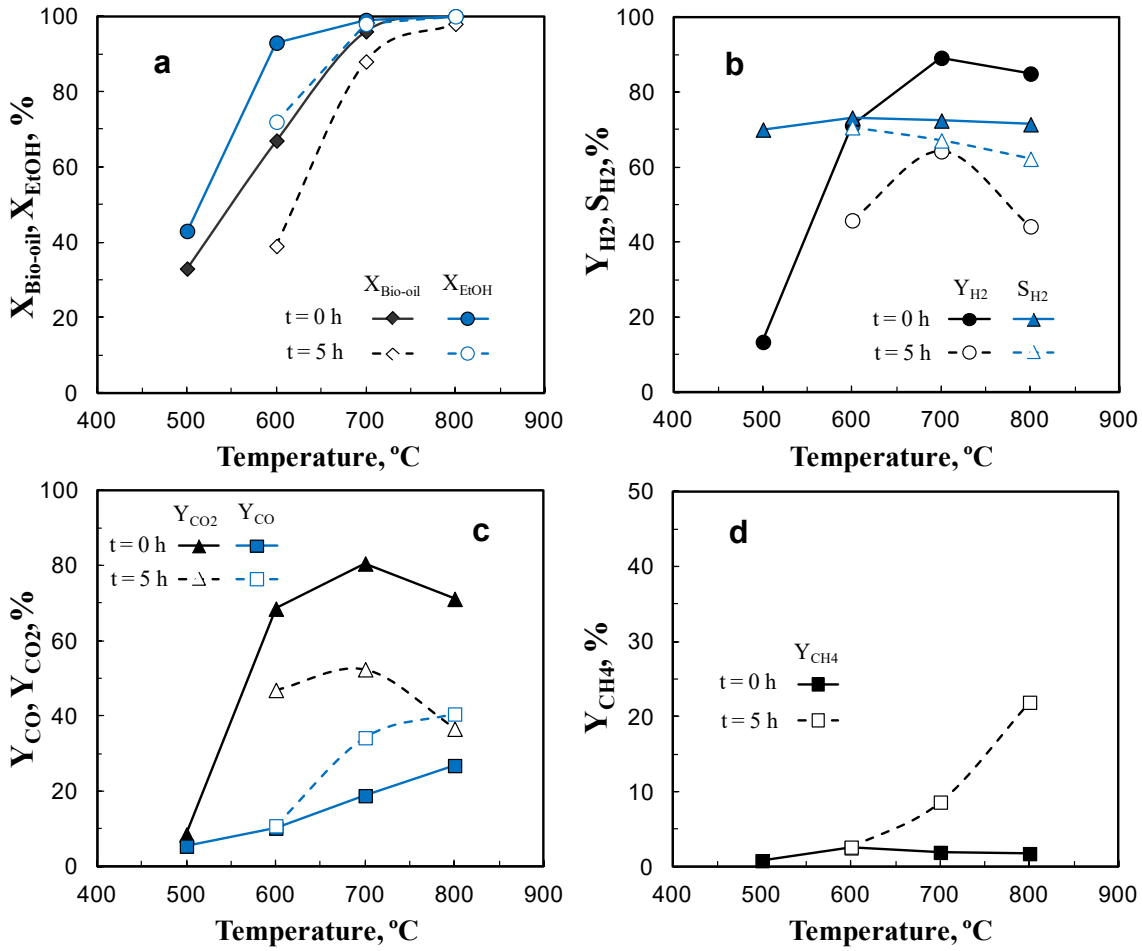
a
b
c
d
$X_{Bio-oil}$, X_{EtOH}, %
Y_{H2}, S_{H2}, %
Y_{CO}, Y_{CO2}, %
Y_{CH4}, %
Temperature, °C
$X_{Bio-oil}$
X_{EtOH}
Y_{H2}
S_{H2}
Y_{CO2}
Y_{CO}
Y_{CH4}
t = 0 h
t = 5 h

Figure 4

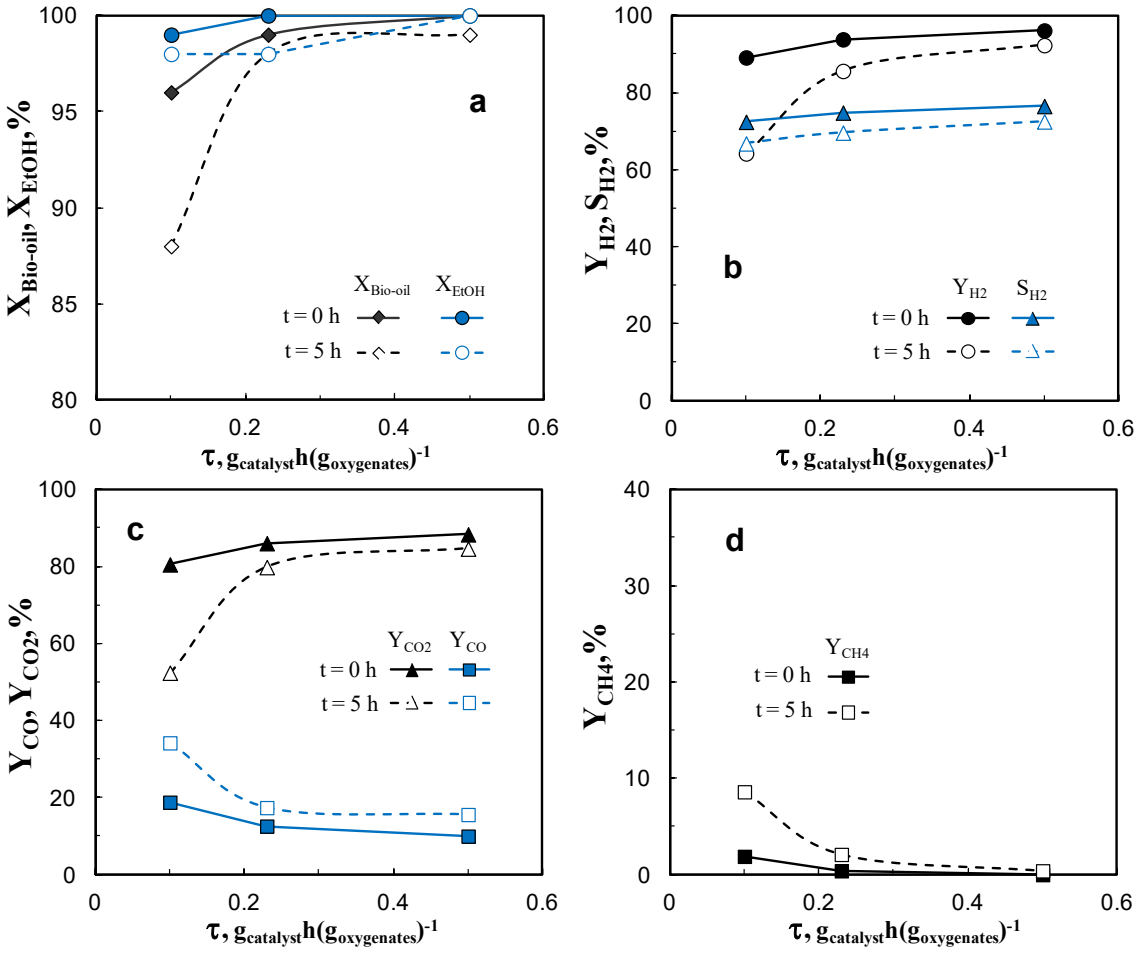
a
b
c
d
$X_{Bio-oil}$, X_{EtOH}, %
Y_{H2}, S_{H2}, %
Y_{CO}, Y_{CO2}, %
Y_{CH4}, %
τ, $g_{catalyst}h(g_{oxygenates})^{-1}$
$X_{Bio-oil}$
X_{EtOH}
Y_{H2}
S_{H2}
Y_{CO2}
Y_{CO}
Y_{CH4}
t = 0 h
t = 5 h

Figure 5

TABLES

Table 1. Composition (wt %) of raw bio-oil (rB), bio-oil aqueous fraction (B) and the mixture with 50 wt% of aqueous ethanol (B_{50}/E_{50}).

Compound/Group	rB	B	B_{50}/E_{50}
Ethanol	0.0	0.0	52.5
Acetic acid	12.8	19.1	9.2
Formic acid	2.1	2.7	1.1
Other acids	1.9	4.7	2.4
Hydroxyacetaldehide	8.5	1.8	0.8
Others aldehydes	6.5	5.5	2.3
Acetone	5.5	1.0	0.5
1-hydroxy-2-propanone	16.3	8.7	3.9
Other ketones	3.8	8.1	4.6
Esters	5.1	3.1	1.3
Ethers	1.4	0.3	0.2
Alcohols	3.7	4.6	2.0
Phenols	16.6	13.4	6.1
Hexose	1.9	2.7	1.6
Levoglucosane	11.0	19.6	9.2
Others	0.4	1.1	0.7
Unidentified	2.5	3.6	1.6

Table 2. Effect of bio-oil/ethanol mass ratio on the values at zero time on stream (fresh catalyst) and after 5 h reaction of bio-oil conversion, ethanol conversion, H_2 yields (catalytic and overall) and reaction products selectivity. Ni/α-Al_2O_3 catalyst, 700º C, S/C = 6-10, $\tau = 0.1\ g_{catalyst}\ h(g_{oxygenates})^{-1}$, $G_{C1}HSV = 41500\ h^{-1}$.

		Bio-oil aqueous fraction/aqueous ethanol (wt%)						
		100/0	**80/20**	**60/40**	**50/50**	**40/60**	**20/80**	**0/100**
Mixture		B_{100}	B_{80}/E_{20}	B_{60}/E_{40}	B_{50}/E_{50}	B_{40}/E_{60}	B_{20}/E_{80}	E_{100}
$X_{Bio\text{-}oil}$	0 h	0.98	0.98	0.96	0.96	0.97	0.99	-
	5 h	0.88	0.92	0.90	0.88	0.96	0.97	-
X_{EtOH}	0 h	-	1	1	1	1	1	1
	5 h	-	0.95	0.97	0.98	0.99	0.99	0.99
$Y_{H2,}$ %	0 h	84.4	88.2	88.9	89.1	89.8	89.2	91.0
	5 h	35.1	49.6	62.5	64.2	73.1	78.9	82.4
$(Y_{H2})^G$, %	0 h	59.3	68.8	74.1	78.1	81.2	84.9	91.0
	5 h	19.0	38.7	52.1	56.4	66.1	75.4	82.4
$S_{H2,}$ %	0 h	68.8	71.6	72.1	72.4	73.0	73.1	72.2
	5 h	47.4	59.9	65.4	67.1	68.8	70.1	71.2
$S_{CO2,}$ %	0 h	26.2	23.7	22.8	21.8	20.9	20.0	19.1
	5 h	11.9	15.3	16.4	16.7	17.7	18.9	18.8
$S_{CO,}$ %	0 h	4.7	4.5	4.8	5.2	5.9	6.7	8.0
	5 h	33.9	19.8	14.4	12.6	10.3	8.9	9
$S_{CH4,}$ %	0 h	0.3	0.2	0.3	0.4	0.2	0.2	0.7
	5 h	5.5	4.3	3.3	3.2	3.0	2.0	1.0
$S_{HCs,}$ %	0 h	0	0	0	0	0	0	0
	5 h	1.3	0.7	0.5	0.4	0.2	0.1	0.1
C_c, wt%		3.8	2.9	1.7	1.3	1.1	0.9	0.5

Table 3. Effect of reforming temperature on coke contents. Conditions: B_{50}/E_{50}, S/C = 7, τ = 0.1 $g_{catalyst}\,h(g_{bio\text{-}oil+EtOH})^{-1}$.

T, ºC	C_c, wt %
500	6.8
600	2.3
700	1.3
800	n.d.

Table 4. Effect of space-time (τ, $g_{catalyst}h(g_{bio\text{-}oil+EtOH})^{-1}$) on coke contents after 5 h of reaction. Conditions: B_{50}/E_{50}, S/C = 7, T = 700 °C.

τ	C_c, wt %
0.10	1.34
0.23	0.65
0.50	n.d.

Comentado [A.R.1]: Añadir columna con TOF